ISSN 1070-3284, Russian Journal of Coordination Chemistry, 2015, Vol. 41, No. 9, pp. 624–628. © Pleiades Publishing, Ltd., 2015.

Insights into the Crystal Structure of a Polyoxomolybdate(VI) Anion Stabilized by Ammonium Cation: Inputs from X-ray Diffraction and Hirshfeld Surface Analysis[1]

X. R. Wu[a], A. Q. Ma[a], F. M. Wang[b], J. Q. Liu[a, *], and A. Kumar[c, **]

[a] *School of Pharmacy, Guangdong Medical University, Dongguan, 523808, P.R. China*

[b] *Department of Chemistry and Chemical Engineering, Shaanxi Xueqian Normal University, Xian 710100, Shannxi, P.R. China*

[c] *Department of Chemistry Faculty of Science, University of Lucknow, Lucknow 226007 India*

*e-mail: *jianqiangliu2010@126.com, **kumar_abhinav@lkouniv.ac.in*

Received January 6, 2015

Abstract—A new polyoxomolybdate complex with chemical formula $[NH_2(CH_3)_2]_4[Mo_8O_{26}]$ (**I**) has been synthesized and structurally characterized. Single-crystal X-ray analysis of compound **I** reveals that the ammonium cation generates an intricate 2D supramolecular architecture (CIF file CCDC no. 1026577). The detail analyses of Hirschfeld surface and fingerprint plots gave a mode of non-covalent interactions in the title compound.

DOI: 10.1134/S1070328415090079

INTRODUCTION

Polyoxometalates (POMs) are discrete metal oxide clusters that are of interest as soluble metal oxides and for applications in catalysis, medicine, and materials science [1–3]. Recently, more and more organic–inorganic hybrid polyoxomolybdate frameworks have been synthesized and characterized [4]. In order to evaluate the nature and energetics associated with intermolecular interactions in the crystal packing, some calculations were performed. The total lattice energy is partitioned into the corresponding Coulombic, polarization, dispersion and repulsion energies [5, 6].

Partitioning is use to evaluate for the corresponding molecular pairs, which contribute towards the understanding of the crystal packing between related molecules. Molecular Hirshfeld surfaces [7] in the crystal structure were constructed on the basis of the electron distribution calculated as the sum of spherical atom electron densities [8, 9]. For a given crystal structure and a set of spherical atomic densities, the Hirshfeld surface is unique [10]. The normalized contact distance (d_{norm}) based on both d_e and d_i (where d_e is distance from a point on the surface to the nearest nucleus outside the surface and d_i is distance from a point on the surface to the nearest nucleus inside the surface) and the vdW radii of the atom, as given by Eq. (1) enables identification of the regions of particular importance to intermolecular interactions [4]. The combination of d_e and d_i in the form of two-dimensional (2D) fingerprint plot [11, 12] provides a summary of intermolecular contacts in the crystal [7]. The Hirshfeld surfaces mapped with d_{norm} and 2D fingerprint plots were generated using the Crystal-Explorer 2.1 [13]. Graphical plots of the molecular Hirshfeld surfaces mapped with d_{norm} used a red-white-blue colour scheme, where red highlight shorter contacts, white represents the contact around vdW separation, and blue is for longer contact. Additionally, two further coloured plots representing shape index and curvedness based on local curvatures are also presented in this paper [14]:

$$d_{norm} = \frac{d_i - r_i^{vdW}}{r_i^{vdW}} + \frac{d_e - r_e^{vdW}}{r_e^{vdW}}. \quad (1)$$

EXPERIMENTAL

Materials and method. All reagents were purchased from commercial sources and used as received. IR spectra were recorded with a Perkin–Elmer Spectrum One spectrometer in the region 4000–400 cm^{-1} using KBr pellets. Thermogravimetric analysis (TGA) was carried out with a Metter–Toledo TA 50 in dry dinitrogen (60 mL min^{-1}) at a heating rate of 5°C min^{-1}.

Synthesis of complex $[NH_2(CH_3)_2]_4[Mo_8O_{26}]$ (I). A mixture of $Zn(OAc)_2 \cdot 2H_2O$ (0.1 mmol), ammonium molybdate (0.1 mmol), 1,3,5-benzenetricarboxylic acid (0.1 mmol), DMF (2 mL) and deionised water (6 mL) was stirred for 30 min in air. The resulting solution was kept at 100°C (oven) for 72 h, and then

[1] The article is published in the original.

Table 1. Crystallographic data and structure refinement for complex **I**

Parameter	Value
Temperature, K	100(2)
Crystal system	Triclinic
Space group	$P\bar{1}$
a, Å	8.7629(5)
b, Å	9.6529(5)
c, Å	10.7201(6)
α, deg	84.968(2)
β, deg	66.090(2)
γ, deg	75.213(2)
Volume, Å^3	801.39(8)
Z	2
ρ_{calcd}, kg/m^3	2.834
F(000)	652
θ Range for data collection, deg	2.61–30.51
Limiting indices hkl	$-11 \le h \le 12$, $-13 \le k \le 13$, $0 \le l \le 15$
Reflections collected	7203
Independent reflections (R_{int})	6344 (0.0313)
Reflections with $I > 2\sigma(I)$	5908
GOOF	1.087
Numbers of paramrtes	215
Final R indices ($I > 2\sigma(I)$)	$R_1 = 0.0241$, $wR_2 = 0.0627$
R indices (all data)	$R_1 = 0.0269$, $wR_2 = 0.0643$
Largest diff. peak and hole, e Å^{-3}	0.982/–0.837

cooled down to 25°C. The resulting crystals formed were filtered off, washed with water and dried in air.

For $C_4H_{16}Mo_4N_2O_{13}$ ($M = 683.95$)

anal. calcd., %:	C, 7.02;	H, 2.36;	N, 4.10.
Found, %:	C, 7.07;	H, 3.31;	N, 4.15.

X-ray crystallography. Single crystal X-ray diffraction analysis of the title compound was carried out on a Bruker SMART APEX II CCD diffractometer equipped with a graphite monochromated MoK_α radiation ($\lambda = 0.71073$ Å) by using ϕ–ω scan technique at room temperature. Data were processed using the Bruker SAINT package and the structures solution and the refinement procedure was performed using SHELX-97 [15]. The structure was solved by direct methods and refined by full-matrix least-squares fitting on F^2. The hydrogen atoms of organic ligands were placed in calculated positions and refined using a riding on attached atoms with isotropic thermal parameters 1.2 times those of their carrier atoms. Table 1 shows crystallographic data of **I**. Selected bond distances and bond angles are listed in Table 2.

Supplementary material for **I** has been deposited with the Cambridge Crystallographic Data Centre (no. 1026577; deposit@ccdc.cam.ac.uk or http://www.ccdc.cam.ac.uk).

RESULTS AND DISCUSSION

The compound crystallizes with an asymmetric unit comprising $[Mo_8O_{26}]^{4-}$ and four ammonium cations $[NH_2(CH_3)_2]^+$ (Fig. 1). The oxygen atoms in the polyoxomolybdate can be classified into four different (O_t, μ_2, μ_3, and μ_4) categories, Mo–O_t 1.702(2)–1.7163(19), Mo–O(μ_2) 1.7409(19)–1.8381(19), Mo–O(μ_3) 1.854(2)–2.359(2), and Mo–O(μ_4) 2.1064(19)–2.494(2) Å. The O(1) taking as μ_2-bridg-

Table 2. Selected bond distances (Å) and angles (deg) for **I**

Bond	d, Å	Bond	d, Å	Bond	d, Å
Mo(1)–O(1)	1.8381(19)	Mo(1)–O(4)	1.9328(19)	Mo(1)–O(2)	1.7754(19)
Mo(2)–O(4)	2.242(2)	Mo(1)–O(3)	1.697(2)	Mo(3)–O(4)	1.8849(19)
Mo(3)–O(5)	2.2317(18)	Mo(2)–O(5)	2.494(2)	Mo(2)–O(6)	1.702(2)
Mo(3)–O(7)	1.7163(19)	Mo(2)–O(8)	1.7409(19)	Mo(4)–O(10)	1.9746(19)
Mo(3)–O(10)	1.9780(19)	Mo(2)–O(10)	2.1818(19)	Mo(4)–O(12)	1.7067(19)
Angle	**ω, deg**	**Angle**	**ω, deg**		
O(2)Mo(1)O(2)	102.66(9)	O(4)Mo(1)O(3)	98.55(9)		
O(2)Mo(1)O(4)	154.06(9)	O(1)Mo(1)O(5)	155.06(9)		
O(9)Mo(2)O(8)	104.86(10)	O(11)Mo(2)O(5)	139.76(8)		
O(8)Mo(2)O(11)	156.66(9)	O(6)Mo(3)O(3)	100.13(10)		
O(7)Mo(3)O(11)	102.25(9)	O(4)Mo(3)O(11)	142.45(8)		
O(11)Mo(4)O(1)	101.39(9)	O(1)Mo(4)O(11)	152.29(9)		

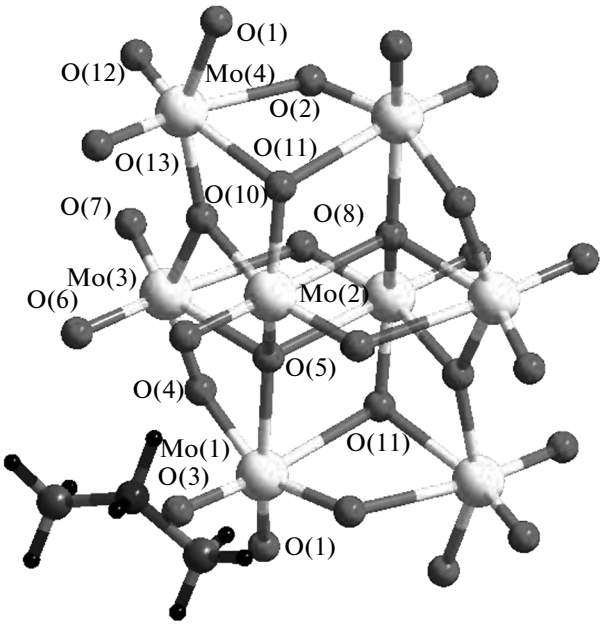

Fig. 1. Coordination environment of Mo^{6+} ions in **I**.

ing mode link the $[Mo_8O_{26}]^{4-}$ subunits into a 1D chain (Fig. 2).

This dimer of ammonium (supramolecular synthon) interacts with the POM cluster through protons on nitrogen, resulting in intricate supramolecular network (Fig. 2) through N(1)···H(1*D*)–O(9), N(1)···H(1*E*)–O(4), N(1)···H(2*E*)–O(7), and N(1)···H(2*D*)–O(13) (symmetry codes: $x + 1$, y, z) interactions having dimensions N···O 2.737(3), 2.841(3), 2.753(3), and 2.797(3) Å, respectively, in the axial position with adjacent POM clusters (Fig. 2). A comparison of the structural characteristics of the title cluster compound with those of reported polyoxomolybdate compounds of $[Zn(HPpz)_3]_2(Mo_8O_{26})$, $[Ni(Bipy)_2]_2(Mo_8O_{26})$, $[Co(H_2Biim)_2(HBiim)]_2$-$(H_2Mo_8O_{26})](H_2O)_4$ clearly reveals that the topology of POMs depends on reaction conditions, stoichiometry, and also on the complex cationic species [16, 17].

The Hirshfeld surfaces of title compound are illustrated in Fig. 3, showing surfaces that have been mapped over a d_{norm} range of –0.5 to 1.5 Å, shape index (–1.0 to 1.0 Å) and curvedness (–4.0 to 0.4 Å). The surfaces are shown as transparent to allow visualization of the aromatic as well as the puckered ring moieties around which they were calculated. The weak interaction information discussed in X-ray crystallography section is summarized effectively in the spots, with the large circular depressions (deep red) visible on the d_{norm} surfaces indicative of hydrogen bonding contacts. The dominant interactions between O–H···O and Mo–O···Mo interactions for the compound can be seen in Hirshfeld surface plots as the bright red shaded area in Fig. 3.

The fingerprint plots for Molybdenum cluster compound are presented in Fig. 4. The O···H and Mo···O intermolecular interactions appear as two distinct spikes of almost equal lengths in the 2D fingerprint plots in the region 2.03 Å < $(d_e + d_i)$ < 2.47 Å as light sky-blue pattern in full fingerprint 2D plots. Complementary regions are visible in the fingerprint plots where one molecule acts as a donor ($d_e > d_i$) and the other as an acceptor ($d_e < d_i$). The fingerprint plots can be decomposed to highlight particular atom pair close contacts. This decomposition enables separation of contributions from different interaction types, which overlap in the full fingerprint. The proportions of O···H interactions comprising 52.4% of the total Hirshfeld surface, while the proportion of Mo···O

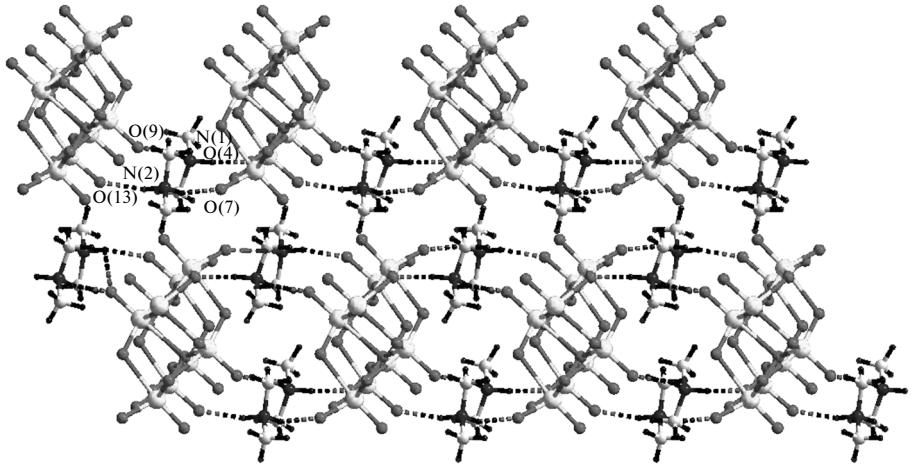

Fig. 2. The 2D supramolecular layer was directed by two different H-bonded interactions among the donor/acceptors sites.

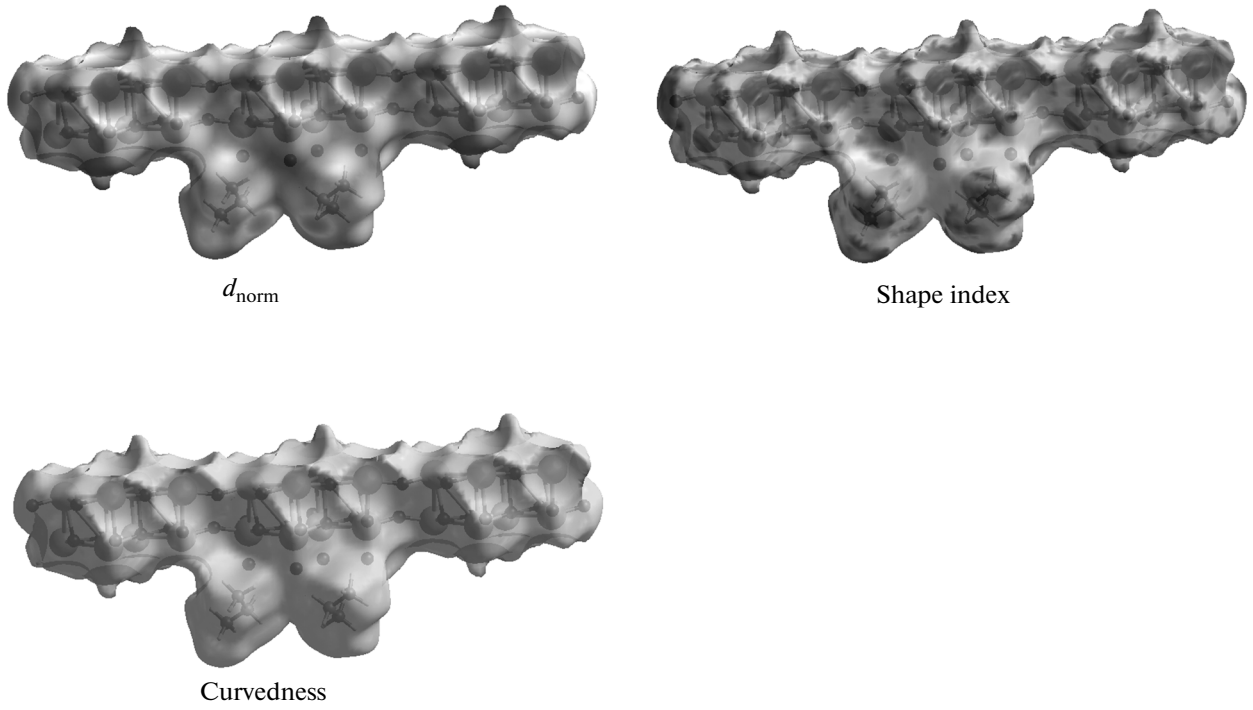

Fig. 3. Hirshfeld surfaces mapped with d_{norm}, shape index and curvedness for the title compound.

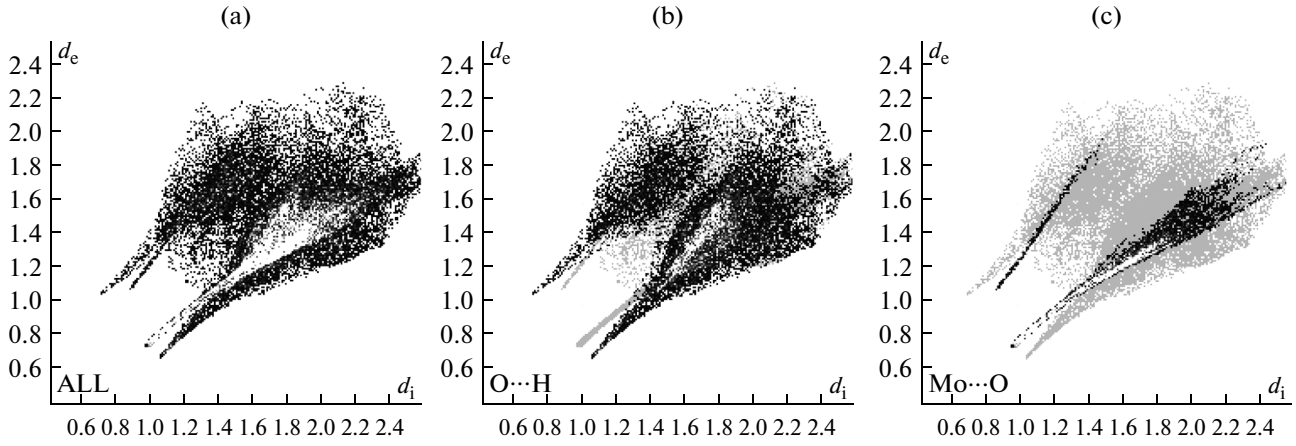

Fig. 4. Fingerprint plots Full (a), resolved into O···H (b) and Mo···O (c) for the Molybdenum cluster compound.

interactions comprises of 25.1% of the total Hirshfeld surface for each molecule of the title compound.

To study the stability of the polymer, TGA of complex **I** was performed (Fig. 5). The compound **I** shows two of weight loss steps. The first weight loss of 13.7% between 20 and 300°C is corresponding to the release of four free water molecules per formula unit (calcd. 13.5%). The second deposition finishes at about 850°C, which can be attributed to the elimination of polyoxomolybdate.

Thus in this study, the role of interacmoelcular interactions of the molecular complex has been analyzed through single crystal motif. The ammonium cations as charge balancing species for anionic polyoxomolybdate act as a supramolecular synthon generating an interesting supramolecular framework. The

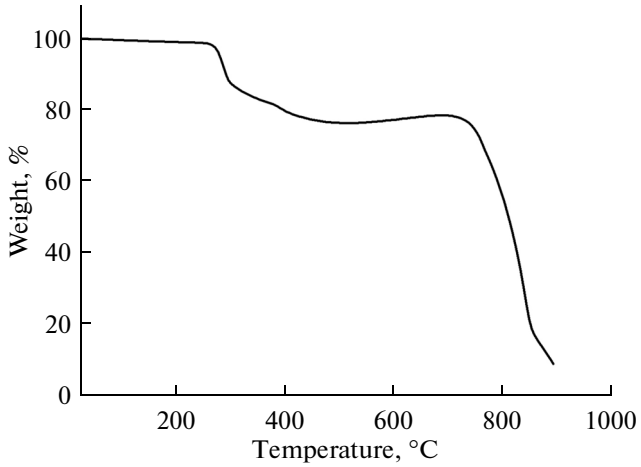

Fig. 5. TG curve of complex **I**.

nature and behaviour of intermolecular interactions were explored through Hirschfeld surface analyses.

ACKNOWLEDGMENTS

The authors acknowledge financial assistance from Guangdong Medical university Research Grants (M2012007) and Thanks for Dr. Zeller Matt for his data collecting.

REFERENCES

1. Long, D.-L. and Tsunashima, R., *Angew. Chem. Int. Ed.*, 2010, vol. 49, p. 1736.
2. Lehn, J.M., *Angew. Chem. Int. Ed.,* 1990, vol. 29, p. 1304.
3. Schulz-Dobrick, M. and Jansen, M., *Inorg. Chem.*, 2007, vol. 46, p. 4380.
4. Kumar, A., Singh, V., Gupta, A.N., et al., *J. Coord. Chem.*, 2012, vol. 65, p. 431.
5. Spackman, M.A. and Jayatilaka, D., *CrystEngComm*, 2009, vol. 11, p. 19.
6. Spackman, M.A. and Byrom, P.G., *Chem. Phys. Lett.*, 1997, vol. 267, p. 215.
7. Spackman, M.A.and McKinnon, J.J., *CrystEngComm*, 2002, vol. 4, p. 378.
8. Spackman, M.A. and Byrom, P.G., *Chem. Phys. Lett.*, 1997, vol. 267, p. 309.
9. McKinnon, J.J., Mitchell, A.S., and Spackman, M.A., *Chem. Eur. J.*, 1998, vol. 4, p. 2136.
10. McKinnon, J.J., Spackman, M.A., and Mitchell, A.S., *Acta Crystallogr., Sect. B: Struct. Sci.*, 2004, vol. 60, p. 627.
11. Rohl, A.L., Moret, M., Kaminsky, W., et al., *Cryst. Growth Des.*, 2008, vol. 8, p. 4517.
12. Parkin, A., Barr, G., Dong, W., et al., *CrystEngComm*, 2007, vol. 9, p. 648.
13. Wolff, S.K., Greenwood, D.J., McKinnon, J.J., et al., *Crystal Explorer, 2.0*, Perth (Australia): Univ. of Western Australia, 2007.
14. Koenderink, J.J. and van Doorn, A.J., *Image Vision Comput.*, 1992, vol. 10, p. 557.
15. Sheldrick, G.M., *SHELXL-97*, Göttingen (Germany): Univ. of Göttingen, 1997
16. Fan, L., Li, D., Wei, P., et al., *J. Coord. Chem.*, 2010, vol. 63, p. 4226.
17. Fan, L.-M., Li, D.-C., Wei, P.-H., et al., *J. Coord. Chem.*, 2011, vol. 64, p. 2531.